Discovery of ^{60}Ca and Implications For the Stability of ^{70}Ca

O. B. Tarasov,[1, 2, 3] D. S. Ahn,[2] D. Bazin,[1] N. Fukuda,[2] A. Gade,[1, 4] M. Hausmann,[5] N. Inabe,[2] S. Ishikawa,[6]
N. Iwasa,[6] K. Kawata,[7] T. Komatsubara,[2] T. Kubo,[5] K. Kusaka,[2] D. J. Morrissey,[1, 8] M. Ohtake,[2]
H. Otsu,[2] M. Portillo,[5] T. Sakakibara,[6] H. Sakurai,[2] H. Sato,[2] B. M. Sherrill,[1, 4] Y. Shimizu,[2] A. Stolz,[1]
T. Sumikama,[2] H. Suzuki,[2] H. Takeda,[2] M. Thoennessen,[1, 4] H. Ueno,[2] Y. Yanagisawa,[2] and K. Yoshida[2]

[1]*National Superconducting Cyclotron Laboratory, Michigan State University, East Lansing, MI 48824, USA*
[2]*RIKEN Nishina Center, RIKEN, 2-1 Hirosawa, Wako, Saitama 351-0198, Japan*
[3]*Flerov Laboratory of Nuclear Reactions, JINR, 141980 Dubna, Moscow Region, Russian Federation*
[4]*Department of Physics and Astronomy, Michigan State University, East Lansing, MI 48824, USA*
[5]*Facility for Rare Isotope Beams, Michigan State University, East Lansing, MI 48824, USA*
[6]*Department of Physics, Tohoku University, 6-3 Aramaki-aza-aoba, Aoba, Sendai 980-8578, Japan*
[7]*Center for Nuclear Study, University of Tokyo, 2-1 Hirosawa, Wako, Saitama 351-0198, Japan*
[8]*Department of Chemistry, Michigan State University, East Lansing, MI 48824, USA*
(Dated: June 11, 2018)

The discovery of the important neutron-rich nucleus $^{60}_{20}$Ca$_{40}$ and seven others near the limits of nuclear stability is reported from the fragmentation of a 345 MeV/u ^{70}Zn projectile beam on ^{9}Be targets at the Radioactive Ion-Beam Factory (RIBF) of the RIKEN Nishina Center. The produced fragments were analyzed and unambiguously identified using the BigRIPS two-stage in-flight separator. The eight new neutron-rich nuclei discovered, ^{47}P, ^{49}S, ^{52}Cl, ^{54}Ar, ^{57}K, ^{59,60}Ca, and ^{62}Sc, are the most neutron-rich isotopes of the respective elements. In addition, one event consistent with ^{59}K was registered. The results are compared with the drip lines predicted by a variety of mass models and it is found that the models in best agreement with the observed limits of existence in the explored region tend to predict the even-mass Ca isotopes to be bound out to at least ^{70}Ca.

Introduction.—The landscape of atomic nuclei is delineated by the nucleon drip lines beyond which no bound states of lighter or heavier isotopes exist. The location of the neutron drip line provides a key benchmark for nuclear models and the quest to understand the nuclear force. Disagreement between model predictions and the actual drip line can reveal missing physics or incorrect assumptions. The heavy oxygen isotopes illustrate such a case where ^{24}O is the last stable isotope, yet the addition of one proton to form fluorine extends the drip line to at least ^{31}F. This unusual behavior has been tied to shell evolution, continuum effects, and many-body forces [1–3]. The next major testing ground that has become accessible to experiments beyond oxygen and fluorine is the calcium isotopic chain [4]. The proton-magic calcium isotopes span the magic neutron numbers 20, 28, 32, 34, and possibly 40 and 50. The calcium chain is just within reach of ab-initio models [3] as well as the broadly applicable mean-field and configuration-interaction models.

Non-relativistic energy density functionals (EDFs) such as [5–8] typically predict the stability of ^{59,60}Ca and some of them, e.g. [5, 6] and the HFB-22,23,26 models in [7], even have ^{70}Ca bound. Shell models based on an effective interaction fitted in the neutron fp shell, such as GXPF1B [9], and relativistic mean-field models [10] also predict the stability of ^{59,60}Ca. In contrast, ab-initio models that include 3N forces and continuum effects predict that ^{59}Ca is unbound [3, 4] and that ^{60}Ca is marginally bound or unbound [11]. Observation of ^{59}Ca

and ^{60}Ca would, therefore, test the predictive power of ab-initio models as compared to EDFs, and indicate if the success of the ab-initio approaches in describing the masses of the calcium isotopes as heavy as ^{54}Ca would allow extrapolation to the drip line.

Measurements at NSCL [12, 13] have demonstrated that the fragmentation of ^{76}Ge and ^{82}Se beams using a two-stage separator can be used to produce new neutron-rich isotopes in the calcium region. We report here the continuation of this work at the RIKEN RIBF facility, using a higher beam energy and intensity, and so accessing the one-order-of-magnitude lower production cross sections needed to explore the stability of ^{59,60}Ca.

Experiment.—A 345 MeV/u ^{70}Zn^{30+} beam delivered by the RIBF accelerator complex was used to irradiate a series of rotating ^{9}Be targets located at the target position of the BigRIPS separator [14]. BigRIPS was operated with full momentum acceptance as a two-stage separator (see Fig.1), where wedge-shaped Al degraders in both stages, at the F1 and F5 dispersive planes, were used to separate and purify the reaction products. The second stage served as a spectrometer for the particle identification (PID) of the reaction products, which was accomplished by measuring time of flight (ToF), energy loss (ΔE), total kinetic energy (TKE), and magnetic rigidity (Bρ) event by event. The PID (Z, A, q) method was described in the appendix of our previous work [15]. The ToF and Bρ measurements and the removal of background events, e.g. from reactions, scattering, or sig-
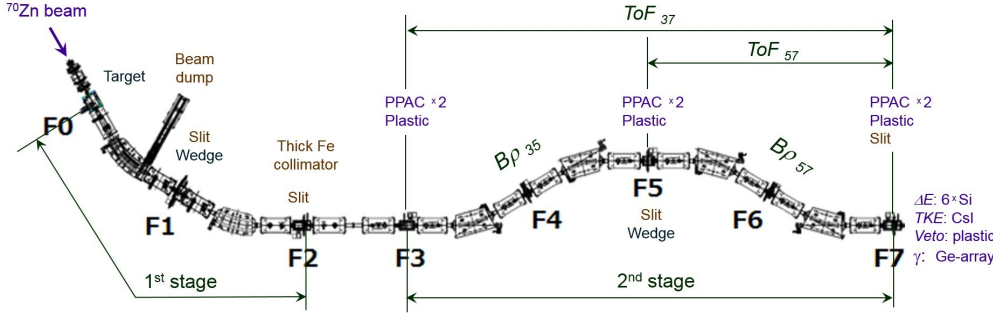
FIG. 1. Schematic layout of the BigRIPS separator. ToF_{37} and ToF_{57} refer to the time-of-flight (ToF) values measured between timing detectors located at F3 and F7, and at F5 and F7, respectively. $B\rho_{35}$ and $B\rho_{57}$ refer to the magnetic rigidity $(B\rho)$ values in the sections from F3 to F5 and from F5 to F7, respectively.

TABLE I. Summary of the experimental conditions for the new isotope search. Five settings of the spectrometer were used, each centered on one exotic isotope.

Settings: isotope tuned	^{50}S	^{53}Cl	^{54}Ar	^{57}K		^{60}Ca	
Be-target thickness (mm)	20	15	10	10		15	
Bρ from 1st dipole (Tm)	7.35	7.8	8.0	8.0		7.35	
Al-wedge thickness at F1, F5 (mm)	3, 3	3, 1	3, 1	3, 1		3, 3	
F2 slit (mm)	± 10	$^{+11}_{-10}$	± 10	± 10	± 10	± 12	
F7 slit (mm)	± 20	± 15	± 15	± 15	± 20	± 20	
Running time (h)	8.9	23.5	11.2	17.0	24.5	14.4	
Intensity (pnA)	231.4	184.4	208.5	190.1	197.3	205.9	
Total rate at F7 (Hz)	11.3	486	536	426	3.9	5.4	
Total number of ^{70}Zn	4.4×10^{16}	9.5×10^{16}	5.0×10^{16}	7.4×10^{16}		2.0×10^{17}	
Main results: ^{A}Z(events)	^{47}P(3),^{54}Ar(2), ^{59}Ca(1)	^{47}P(6),^{49}S(1), ^{54}Ar(2)	^{47}P(3),^{49}S(3), ^{52}Cl(1),^{54}Ar(1)	^{49}S(1),^{52}Cl(1), ^{54}Ar(4),^{57}K(1)		^{54}Ar(4),^{57}K(6),^{59}K(1), ^{59}Ca(6),^{60}Ca(2),^{62}Sc(2)	

nal pileup, were done as in previous BigRIPS experiments [16–18]. The particles of interest were stopped in a 76-mm thick CsI crystal after passing through six 1-mm thick silicon PIN diodes. The ΔE signals from all six Si detectors were used for the Z determination and to exclude inconsistent events. A thick plastic scintillator positioned behind the CsI detector served as a veto against light products from reactions in upstream detectors. Bρ measurements in both halves of the second stage allowed us to deduce $B\rho_{35}$ and $B\rho_{57}$ for the fragments before and after the energy degrader placed at the momentum-dispersive focus F5. The Bρ of the fragments was reconstructed from position and angle measurements at each of the F3, F5, and F7 foci using two sets of position-sensitive parallel plate avalanche counters (PPACs). Table I summarizes the experimental conditions for the new isotope search. All settings, including the target and degrader thicknesses as well as slit widths at F2 and F7, were optimized with the LISE^{++} simulation code [19] to obtain the maximum production rate of new isotopes, while limiting the counting rates to less than 500 kHz at F3 and about 1 kHz at F7.
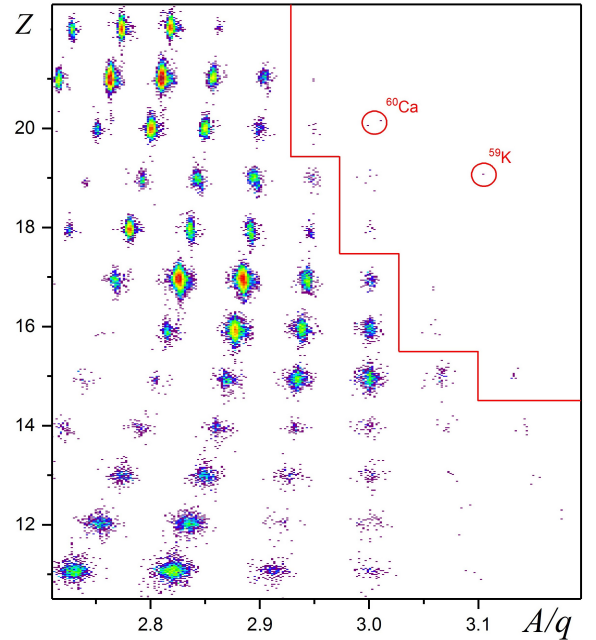

FIG. 2. Z versus A/q PID plot for nuclei observed in the measurement reported here. The limit of previously observed nuclei is indicated by the red solid line.
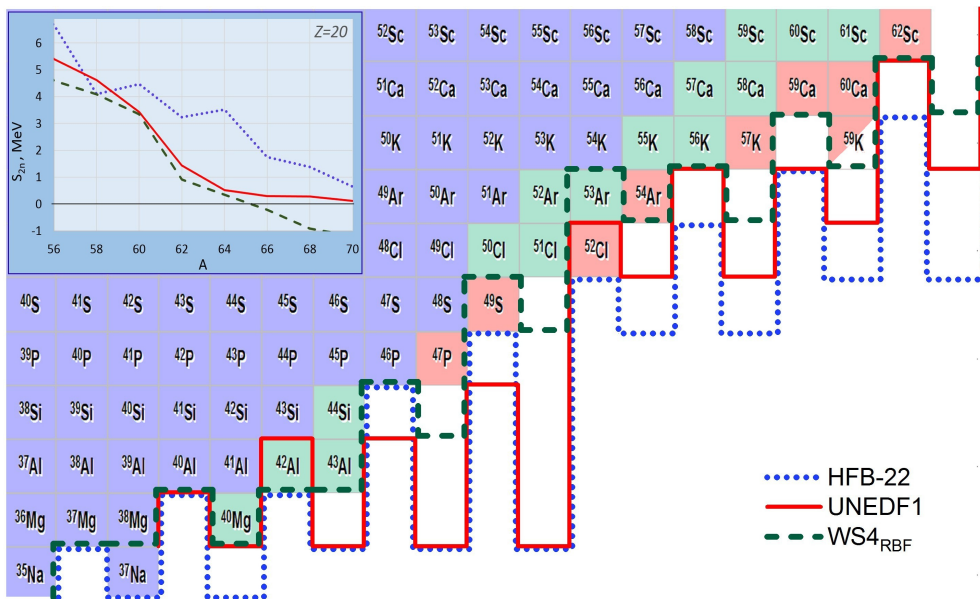
FIG. 3. The region of the chart of nuclides studied in this work. Nuclei highlighted by red background were discovered in this work, green squares denote nuclei discovered at the NSCL since 2007 [12, 13, 20, 21]. The neutron drip lines predicted by the HFB-22 [7], UNEDF1 [22], and WS4$_{RBF}$ [23] mass models are indicated by the blue dotted, red solid, and green dashed lines, respectively. The model WS4$_{RBF}$ appears to underestimate the bindings of isotopes in this region. HFB-22 and UNEDF1 seem to better predict the drip line. The inset shows the predicted S$_{2n}$ values for even neutron-rich calcium isotopes.

Results.—Figure 2 shows the PID plot (Z vs. A/q) for the data from all settings in Table I, totaling 99.5 hours of beam on target at an average ^{70}Zn beam current of 198.6 pnA. The observed fragments include eight new isotopes that are the most neutron-rich nuclides of the elements from phosphorus to scandium, ^{47}P (12), ^{49}S (5), ^{52}Cl (2), ^{54}Ar (13), ^{57}K (8), ^{59}Ca (9), ^{60}Ca (2), ^{62}Sc (2) (the number of detected events is given in brackets). One event consistent with ^{59}K was observed as well. The events corresponding to these new neutron-rich nuclei are indicated to the right of the red solid line in Fig. 2.

The increased beam intensity ($\times 5$) and target thickness ($\times 4$) relative to our previous work in this region [13, 15] afforded sensitivity to subfemto-barn cross sections. For example, the production cross sections of ^{59}Ca and ^{60}Ca were determined to be $8(\pm 3) \times 10^{-16}$ and $2.1(\pm 1.5) \times 10^{-16}$ barn, respectively, close to the estimates [13] from the LISE^{++} abrasion-ablation model and the Q_g-systematics, with masses calculated with the GXPF1B5 shell-model interaction [9, 13]. The ^{60}Ca production exceeds the prediction based on EPAX 3 [24] by a factor of 10. The production cross sections and momentum distributions for all neutron-rich nuclei observed here will be the subject of a forthcoming publication [25]. Of special note are two points: (i) the observation of ^{62}Sc at these beam energies and with a light target, for which the production involves a net 9 proton stripping and one neutron pick-up and (ii) the non-observation of ^{55}Ar, that had an expected yield of 3^{+2}_{-1} counts based on Q_g-systematics [20] and yields measured here. This corresponds to a $95.0^{+4.3}_{-8.6}\%$ probability (Poisson statistics) of the unobserved isotope being unbound.

Discussion.— The observation of ^{59,60}Ca demonstrates that the ab-intio models [3] that predict them unbound are missing aspects that lead to more binding for neutron-

rich nuclei. Certain other models do better at reproducing the new isotopes observed in this study. We compare the observation of particle stability in the neutron-rich region for the elements with $11 \leq Z \leq 21$ with the predictions of a number of mass models. In a first step, 35 mass models and mass tables were considered: AME mass tables [26, 27] with extrapolations using the LISE^{++} liquid-drop model (LDM1) [28], the Weizsäcker-Skyrme (WS) [23] and finite-range droplet (FRDM) [29, 30] macroscopic-microscopic mass formulas, the TUYY and KTUY empirical mass formulas [31, 32], a series of non-relativistic Hartree-Fock-Bogoliubov (HFB) mass models (HFB-9,17,21-32 [6–8, 33, 34], six of the EDFs discussed in [5] and the Gogny-HFB model [35]), relativistic mean-field (RMF) models [10], and a shell model based on effective interactions fitted in the neutron fp shell GXPF1B and GXPF1B5 [9, 13]. The nuclides ^{36}Na and ^{39}Mg, which are known to be neutron-unbound, and observed neutron-bound isotopes, including ^{49}S and ^{52}Cl reported here for the first time as well as ^{37}Mg, ^{40,42}Al, ^{53}Ar, were used to select a subset of models that describe the particle stability in this region reasonably well. We note that complete agreement with our bound/unbound benchmarks listed above was only achieved for the HFB-22 functional [7] and UNEDF0 [36]. Fig. 3 shows the neutron drip lines predicted by three models, HFB-22, UNEDF1 [22] and WS4$_{RBF}$, and illustrates the large variation in their predictions. The macroscopic-microscopic WS4$_{RBF}$ [23] model was chosen for comparison since it has the lowest rms deviation of 298 keV with respect to available mass data, but as can be seen, it does not extrapolate well. We note, that both HFB-22 and the UNEDF0 functional, which describe the experimentally established limits of existence in the explored region well, also predict the even-mass Ca isotopes to be bound up
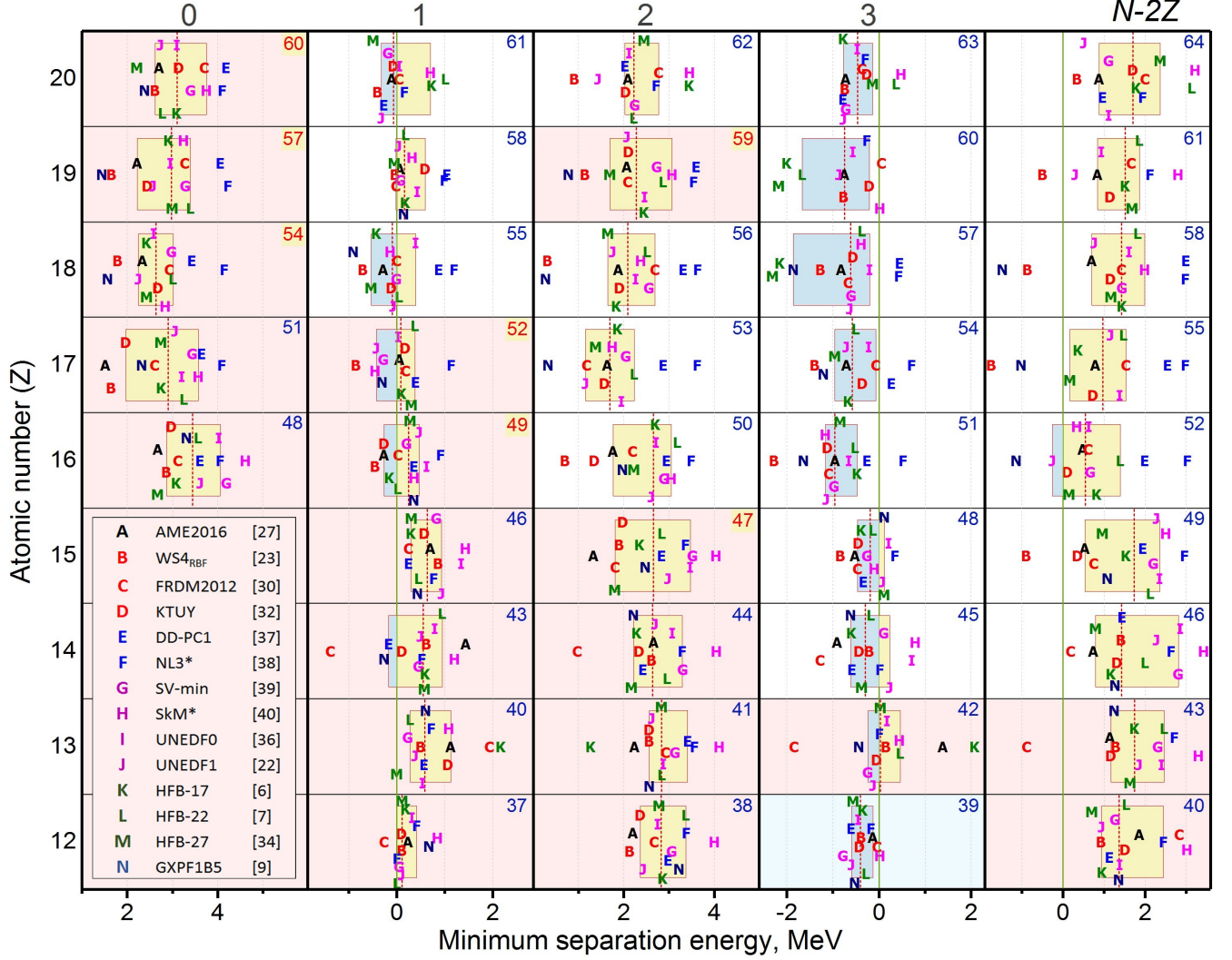
FIG. 4. Compilation of the minimum neutron separation energy for a variety of mass models arranged by Z vs. $N-2Z$. The mass number, A, is shown in the top right corner of each isotope cell. The mass numbers of newly discovered isotopes are indicated in red. Red(blue) background color for a cell indicates that the isotope has been observed to be bound(unbound) and white color indicates an unknown status. The rectangle in each cell is the $<20,80>$ model distribution percentile, where yellow background color symbolizes particle bound and blue color particle-unbound. Medians are shown as vertical red dashed lines. Macroscopic-microscopic mass formulas (B-D) are indicated by red letters, the RMF models [10] (E,F) by blue letters, Erler's EDF family [5] (G-J) by pink letters, BsK functionals of the HFB family [7] (K-M) by green letters, and the shell model by a dark blue N, respectively.

to at least ^{70}Ca (see Fig. 3 inset), in contradiction with predictions from ab-initio models that found the neutron drip line closer to ^{60}Ca.

Figure 3 provides limited information for a few models. In order to provide a more detailed picture, 14 mass models, spanning the different families of models listed, were selected for a more detailed comparison. Fig. 4 shows the predicted minimum neutron separation energy, $\min(S_{1n}, S_{2n})$, for isotopes of Na to Ca with $N-2Z$ ranging from 0 to 4. The newly observed ^{49}S and ^{52}Cl isotopes can be taken as an interesting discriminator with

the spread in the model predictions ranging from unbound to bound. As expected for models that largely rely on parameterizations deduced from fits to masses closer to stability, the spread in the model predictions becomes wider towards the more neutron-rich systems. Curiously, the spread in the predicted values is smallest for the neutron-odd systems characterized by $N-2Z=1$ and 3. Based on Fig. 4, the neutron-odd isotopes along the $N-2Z=1$ line of elements $18 \leq Z \leq 20$ emerge as interesting future targets for new isotope searches. ^{61}Ca will be of special interest as in the normal-order filling

of shells, the $\nu g_{9/2}$ orbital must be occupied at $N = 41$. Bound ^{70}Ca would indicate that the $\nu g_{9/2}$ orbital stays at least weakly bound out to ^{70}Ca, with pairing possibly deciding on the fate of the odd-A Ca isotopes.

Summary.—The discovery of $^{60}_{20}$Ca$_{40}$ and seven other neutron-rich nuclei near the limits of stability is reported from the projectile fragmentation of a 345 MeV/u primary ^{70}Zn beam on Be targets at the RI Beam Factory operated by RIKEN Nishina Center and CNS, University of Tokyo. During a 99.5 hour measurement, ^{47}P, ^{49}S, ^{52}Cl, ^{54}Ar, ^{57}K, ^{59,60}Ca, and ^{62}Sc, the most neutron-rich isotopes of the respective elements, were observed for the first time. In addition, one event consistent with ^{59}K was observed. The results are compared with the drip-line predictions of a wide variety of mass models. The two isotopes ^{49}S and ^{52}Cl, discovered in this work, emerge as key discriminators between different models. The energy density functionals in best agreement with the limits of existence in the explored region, HFB-22 and UNEDF0, predict the even-mass Ca isotopes to be bound out to at least ^{70}Ca, at odds with ab-initio models that predict the neutron drip line in Ca to be closer to ^{60}Ca with ^{59}Ca unbound.

[1] T. Otsuka, T. Suzuki, J. D. Holt, A. Schwenk, and Y. Akaishi, Phys. Rev. Lett. **105**, 032501 (2010).

[2] G. Hagen, M. Hjorth-Jensen, G. R. Jansen, R. Machleidt, and T. Papenbrock, Phys. Rev. Lett. **108**, 242501 (2012).

[3] G. Hagen, M. Hjorth-Jensen, G. R. Jansen, R. Machleidt, and T. Papenbrock, Phys. Rev. Lett. **109**, 032502 (2012).

[4] C. Forssén, G. Hagen, M. Hjorth-Jensen, W. Nazarewicz, and J. Rotureau, Phys. Scr. **T152**, 014022 (2013).

[5] J. Erler, N. Birge, M. Kortelainen, W. Nazarewicz, E. Olsen, A. M. Perhac, and M. Stoitsov, Nature **486**, 509 (2012).

[6] S. Goriely, N. Chamel, and J. M. Pearson, Phys. Rev. Lett. **102**, 152503 (2009).

[7] S. Goriely, N. Chamel, and J. M. Pearson, Phys. Rev. C **88**, 024308 (2013).

[8] S. Goriely, N. Chamel, and J. M. Pearson, Phys. Rev. C **93**, 034337 (2016).

[9] Y. Utsuno, T. Otsuka, B. A. Brown, M. Honma, T. Mizusaki, and N. Shimizu, Phys. Rev. C **86**, 051301(R) (2012).

[10] S. E. Agbemava, A. V. Afanasjev, D. Ray, and P. Ring, Phys. Rev. C **89**, 054320 (2014).

[11] G. Hagen, P. Hagen, H.-W. Hammer, and L. Platter, Phys. Rev. Lett. **111**, 132501 (2013).

[12] O. B. Tarasov, D. J. Morrissey, A. M. Amthor, T. Baumann, D. Bazin, A. Gade, T. N. Ginter, M. Hausmann, N. Inabe, T. Kubo, A. Nettleton, J. Pereira, M. Portillo, B. M. Sherrill, A. Stolz, and M. Thoennessen, Phys. Rev. Lett. **102**, 142501 (2009).

[13] O. B. Tarasov, M. Portillo, D. J. Morrissey, A. M. Amthor, L. Bandura, T. Baumann, D. Bazin, J. S. Berryman, B. A. Brown, G. Chubarian, N. Fukuda, A. Gade, T. N. Ginter, M. Hausmann, N. Inabe, T. Kubo, J. Pereira, B. M. Sherrill, A. Stolz, C. Sumithrarachchi, M. Thoennessen, and D. Weisshaar, Phys. Rev. C **87**, 054612 (2013).

[14] T. Kubo, Nucl. Instrum. Meth. Phys. Res. B **204**, 97 (2003).

[15] O. B. Tarasov, M. Portillo, A. M. Amthor, T. Baumann, D. Bazin, A. Gade, T. N. Ginter, M. Hausmann, N. Inabe, T. Kubo, D. J. Morrissey, A. Nettleton, J. Pereira, B. M. Sherrill, A. Stolz, and M. Thoennessen, Phys. Rev. C **80**, 034609 (2009).

[16] T. Ohnishi, T. Kubo, K. Kusaka, A. Yoshida, K. Yoshida, N. Fukuda, M. Ohtake, Y. Yanagisawa, H. Takeda, D. Kameda, Y. Yamaguchi, N. Aoi, K. I. Yoneda, H. Otsu, S. Takeuchi, T. Sugimoto, Y. Kondo, H. Scheit, Y. Gono, H. Sakurai, T. Motobayasi, H. Suzuki, T. Nakao, H. Kimura, Y. Mizo, M. Matsushita, K. Ieki, T. Kuboki, T. Yamaguchi, T. Suzuki, A. Ozawa, T. Moriguchi, Y. Yasuda, T. Nakamura, T. Nannichi, T. Shimamura, Y. Nakayama, H. Geissel, H. Weick, J. A. Nolen, O. B. Tarasov, A. S. Nettleton, D. P. Bazin, B. M. Sherrill, D. J. Morrissey, and W. Mittig, J. Phys. Soc. Jpn. **77**, 083201 (2008).

[17] H. Suzuki, T. Kubo, N. Fukuda, N. Inabe, D. Kameda, H. Takeda, K. Yoshida, K. Kusaka, Y. Yanagisawa, M. Ohtake, H. Sato, Y. Shimizu, H. Baba, M. Kurokawa, K. Tanaka, O. B. Tarasov, D. Bazin, D. J. Morrissey, B. M. Sherrill, K. Ieki, D. Murai, N. Iwasa, A. Chiba, Y. Ohkoda, E. Ideguchi, S. Go, R. Yokoyama, T. Fujii, D. Nishimura, H. Nishibata, S. Momota, M. Lewitowicz, G. DeFrance, I. Celikovic, and K. Steiger, Phys. Rev. C **96**, 034604 (2017).

[18] N. Fukuda, T. Kubo, D. Kameda, N. Inabe, H. Suzuki, Y. Shimizu, H. Takeda, K. Kusaka, Y. Yanagisawa, M. Ohtake, K. Tanaka, K. Yoshida, H. Sato, H. Baba, M. Kurokawa, T. Ohnishi, N. Iwasa, A. Chiba, T. Yamada, E. Ideguchi, S. Go, R. Yokoyama, T. Fujii, H. Nishibata, K. Ieki, D. Murai, S. Momota, D. Nishimura, Y. Sato, J. Hwang, S. Kim, O. B. Tarasov, D. J. Morrissey, and G. Simpson, J.Phys.Soc.Jpn. **87**, 014202 (2018).

[19] O. B. Tarasov and D. Bazin, Nucl. Inst. Meth. B **266**, 4657 (2008), http://lise.nscl.msu.edu.

[20] O. B. Tarasov, T. Baumann, A. M. Amthor, D. Bazin, C. M. Folden III, T. N. Ginter, M. Hausmann, M. Matos, D. J. Morrissey, A. Nettleton, M. Portillo, A. Schiller, B. M. Sherrill, A. Stolz, and M.Thoennessen, Phys. Rev. C **75**, 064613 (2007).

[21] T. Baumann, A. M. Amthor, D. Bazin, B. A. Brown, C. M. Folden III, A. Gade, T. N. Ginter, M. Hausmann, M. Matos, D. J. Morrissey, M. Portillo, A. Schiller, B. M. Sherrill, A. Stolz, O. B. Tarasov, and M. Thoennessen, Nature **449**, 1022 (2007).

[22] M. Kortelainen, J. McDonnell, W. Nazarewicz, P.-G. Reinhard, J. Sarich, N. Schunck, M. V. Stoitsov, and S. M. Wild, Phys. Rev. C **85**, 024304 (2012).

[23] N. Wang, M. Liu, X. Wu, and J. Meng, Phys. Lett. B **734**, 215 (2014).

[24] K. Sümmerer, Phys. Rev. C **86**, 014601 (2012).

[25] O. B. Tarasov and et al., in preparation (2018).

[26] M. Wang, G. Audi, A. H. Wapstra, F. G. Kondev, M. MacCormick, X. Xu, and B. Pfeiffer, Chinese Physics C **36**, 1603 (2012).

[27] M. Wang, G. Audi, F. G. Kondev, W. J. Huang, S. Naimi, and X. Xu, Chinese Physics C **41**, 030003 (2017).

[28] O. B. Tarasov and D. Bazin, *LISE*$^{++}$: *design your own spectrometer*, Tech. Rep. MSUCL1248 (NSCL, MSU, 2002).

[29] P. Möller, J. R. Nix, W. D. Myers, and W. J. Swiatecki, At. Data Nucl. Data Tables **59**, 185 (1995).

[30] P. Möller, W. D. Myers, H. Sagawa, and S. Yoshida, Phys. Rev. Lett. **108**, 052501 (2012).

[31] T. Tachibana, M. Uno, M. Yamada, and S. Yamada, At. Data Nucl. Data Tables **39**, 185 (1988).

[32] H. Koura, T. Tachibana, M. Uno, and M. Yamada, Prog. Theo. Phys. **113**, 305 (2005).

[33] S. Goriely, M. Samyn, J. M. Pearson, and M. Onsi, Nucl. Phys. A **750**, 425 (2005).

[34] S. Goriely, N. Chamel, and J. M. Pearson, Phys. Rev. C **88**, 061302(R) (2013).

[35] S. G. S. Hilaire, M. Girod, and S. Péru, Phys. Rev. Lett. **102**, 242501 (2009).

[36] M. Kortelainen, T. Lesinski, J. More, W. Nazarewicz, J. Sarich, N. Schunck, M. V. Stoitsov, and S. Wild, Phys. Rev. C **82**, 024313 (2010).

[37] T. Nikšić, D. Vretenar, and P. Ring, Phys. Rev. C **78**, 034318 (2008).

[38] G. A. Lalazissis, S. Karatzikos, R. Fossion, D. P. Arteaga, A. V. Afanasjev, and P. Ring, Phys. Lett. B **671**, 36 (2009).

[39] P. Klüpfel, P.-G. Reinhard, T. J. Brvenich, and J. A. Maruhn, Phys. Rev. C **79**, 034310 (2009).

[40] J. Bartel, P. Quentin, M. Brack, C. Guet, and H.-B. Håkansson, Nucl. Phys. A **386**, 79 (1982).